

See discussions, stats, and author profiles for this publication at: <https://www.researchgate.net/publication/230709194>

# Structure–Reactivity Relationships and Intrinsic Reaction Barriers for Nucleophile Additions to a Quinone Methide: A Strongly Resonance–Stabilized Carbocation

ARTICLE *in* JOURNAL OF THE AMERICAN CHEMICAL SOCIETY · MARCH 2000

Impact Factor: 12.11 · DOI: 10.1021/ja9937526

---

CITATIONS

67

---

READS

47

3 AUTHORS, INCLUDING:



[John P. Richard](#)

University at Buffalo, The State University of ...

219 PUBLICATIONS 6,902 CITATIONS

[SEE PROFILE](#)



[Juan Crueiras](#)

University of Santiago de Compostela

38 PUBLICATIONS 388 CITATIONS

[SEE PROFILE](#)

# Structure–Reactivity Relationships and Intrinsic Reaction Barriers for Nucleophile Additions to a Quinone Methide: A Strongly Resonance-Stabilized Carbocation

John P. Richard,<sup>\*,†,1a</sup> Maria M. Toteva,<sup>†</sup> and Juan Crujeiras<sup>‡,1b</sup>

Contribution from the Department of Chemistry, University at Buffalo, SUNY, Buffalo New York 14260-3000, and the Departamento de Química Física, Facultad de Química, Universidad de Santiago, 15706 Santiago de Compostela, Spain

Received October 19, 1999

**Abstract:** Second-order rate constants  $k_{\text{Nu}}$  ( $\text{M}^{-1} \text{s}^{-1}$ ) were determined for addition of a wide range of nucleophiles to the simple quinone methide 4-[bis(trifluoromethyl)methylene]cyclohexa-2,5-dienone (**1**) to give the nucleophile adduct **1-Nu** in water. Equilibrium constants were determined for the overall addition of HBr and HI to **1** to give **H-1-Nu**, and the data were used to calculate equilibrium constants for the addition of  $\text{Br}^-$  and  $\text{I}^-$  to **1**, and to estimate equilibrium constants for the addition of  $\text{Cl}^-$  and  $\text{AcO}^-$ . The values of  $\log k_{\text{Nu}}$  show a linear correlation with the Ritchie nucleophilicity parameter  $N_+$  with a slope  $s = 0.92 \pm 0.10$  that is essentially the same as the electrophile-independent value of 1.0 for highly resonance-stabilized carbocations. Marcus intrinsic barriers  $\Delta$  of 12.4, 13.9, 15.4, and 19.8 kcal/mol are reported for the addition of  $\text{I}^-$ ,  $\text{Br}^-$ ,  $\text{Cl}^-$ , and  $\text{AcO}^-$  to **1**, respectively. The thermodynamic barriers  $\Delta G^\circ$  and intrinsic barriers  $\Delta$  for addition of  $\text{Br}^-$ ,  $\text{Cl}^-$ , and  $\text{AcO}^-$  to **1** are  $8.4 \pm 1.0$  and  $5.2 \pm 0.2$  kcal/mol larger, respectively, than the corresponding barriers for addition of these nucleophiles to the triphenylmethyl carbocation. It is concluded that, by the criterion of its chemical reactivity, **1** behaves as a highly resonance-stabilized carbocation. Values of  $N_+ = 4.0, 2.2, 1.2$  and  $0.60$ , respectively, are reported for  $\text{I}^-$ ,  $\text{Br}^-$ ,  $\text{Cl}^-$ , and  $\text{AcO}^-$ , which do not form stable adducts to Ritchie electrophiles. The slope of 2.0 ( $r = 0.98$ ) for the linear correlation between Ritchie ( $N_+$ ) and Swain–Scott ( $n$ ) nucleophilicity parameters shows that there is substantially greater bonding between the nucleophile and carbon at the transition state for nucleophile addition to  $\text{sp}^2$ -hybridized carbon than for addition to  $\text{sp}^3$ -hybridized carbon. Azide ion and nucleophiles with a nonbonding electron pair(s) at atoms adjacent to the nucleophilic site ( $\alpha$ -effect nucleophiles) exhibit significant positive deviations from this correlation.

## Introduction

Quinone methides are a class of organic compounds with considerable importance in chemistry and biology.<sup>2–14</sup> The

structure of quinone methides invites comparisons with better characterized organic functional groups. For example, simple quinone methides may be thought of as very highly stabilized *p*-alkoxy substituted benzylic carbocations (Scheme 1, **A**) or as examples of cyclic Michael acceptors (**B**). However, a definitive classification is difficult because of the relative lack of data on the chemical and physical properties of quinone methides.

We have reported methods for generation of the simple quinone methide 4-[bis(trifluoromethyl)methylene]cyclohexa-2,5-dienone (**1**),<sup>15</sup> and the results of a study of the uncatalyzed and specific-acid-catalyzed addition of halide ions to **1** in a solvent of 50/50 (v/v) trifluoroethanol/water.<sup>16</sup> We have now extended this work and report here the results of a study of the reaction of **1** with a large number of nucleophilic reagents in water. These studies were undertaken for the following reasons:

(1) We have treated<sup>15,16</sup> quinone methides as members of the class of strongly resonance-stabilized benzylic carbocations (Scheme 1, **A**), and others have also found this classification to be useful.<sup>7,17</sup> A principal goal of this work was to compare the reactivity of quinone methides and carbocations, to determine

<sup>†</sup> University at Buffalo, SUNY.

<sup>‡</sup> Universidad de Santiago.

(1) (a) Tel: (716) 645 6800 ext 2194. Fax: (716) 645 6963. Email: jrichard@chem.buffalo.edu. (b) Current Address: Departamento de Química Física, Facultad de Química, Universidad de Santiago, 15706 Santiago de Compostela, Spain.

(2) Angle, S. R.; Arnaiz, D. O.; Boyce, J. P.; Frutos, R. P.; Louie, M. S.; Mattson-Arnaiz, H. L.; Rainier, J. D.; Turnbull, K. D.; Yang, W. J. *Org. Chem.* **1994**, *59*, 6322–6337.

(3) Angle, S. R.; Rainier, J. D.; Woytowicz, C. J. *Org. Chem.* **1997**, *62*, 5884–5892.

(4) Boruah, R. C.; Skibo, E. B. *J. Org. Chem.* **1995**, *60*, 2232–2243.

(5) Dorrestijn, E.; Pugin, R.; Nogales, M. V. C.; Mulder, P. J. *Org. Chem.* **1997**, *62*, 4804–4810.

(6) Gaudiano, G.; Frigerio, M.; Sangsurasak, C.; Bravo, P.; Koch, T. H. *J. Am. Chem. Soc.* **1992**, *114*, 5546–5553.

(7) McCracken, P. G.; Bolton, J. L.; Thatcher, G. R. J. *J. Org. Chem.* **1997**, *62*, 1820–1825.

(8) Myers, J. K.; Cohen, J. D.; Widlanski, T. S. *J. Am. Chem. Soc.* **1995**, *117*, 11049–11054.

(9) Paul, G. C.; Gajewski, J. J. *J. Org. Chem.* **1993**, *58*, 5060–5062.

(10) Pande, P.; Shearer, J.; Yang, J.; Greenberg, W.; Rokita, S. E. *J. Am. Chem. Soc.* **1999**, *121*, 6773–6779.

(11) Tomasz, M.; Das, A.; Tang, K. S.; Ford, M. G. J.; Minnock, A.; Musser, S. M.; Waring, M. J. *J. Am. Chem. Soc.* **1998**, *120*, 11581–11593.

(12) Trahanovsky, W. S.; Chou, C.-H.; Fischer, D. R.; Gerstein, B. C. *J. Am. Chem. Soc.* **1988**, *110*, 6579–6581.

(13) Wan, P.; Barker, B.; Diao, L.; Fisher, M.; Shi, Y.; Yang, C. *Can. J. Chem.* **1996**, *74*, 465–475.

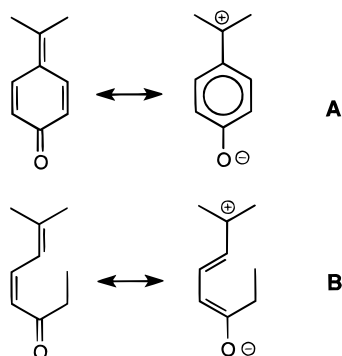
(14) Fischer, M.; Wan, P. *J. Am. Chem. Soc.* **1998**, *120*, 2680–2681.

(15) Richard, J. P.; Amyes, T. L.; Bei, L.; Stubblefield, V. *J. Am. Chem. Soc.* **1990**, *112*, 9513–9519.

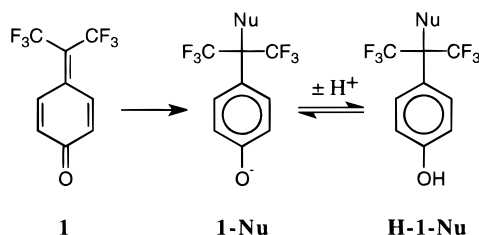
(16) Richard, J. P. *J. Am. Chem. Soc.* **1991**, *113*, 4588–4595.

(17) Hulbert, P. B.; Glover, P. L. *Biochem. Biophys. Res. Commun.* **1983**, *117*, 129–134.

Scheme 1



Scheme 2



whether, by the criterion of its chemical reactivity, **1** behaves as a member of the larger class of strongly resonance-stabilized carbocations.

(2) There have been few measurements of rate and equilibrium constants for addition of halide ions to weakly reactive electrophiles, because these anions do not form stable adducts to such electrophiles. The adducts of halide ions to **1** (**1-Nu**, Scheme 2) are likewise unstable; however, rate and equilibrium data for their formation can be obtained by coupling nucleophile addition to protonation of the phenoxide oxygen of **1-Nu** to give **H-1-Nu** (Scheme 2).<sup>16</sup> We report here rate and equilibrium data for the addition of halide and acetate ions to **1**, which allows for extension to these nucleophiles of the well-known Ritchie  $N_+$  relationship for carbocation–nucleophile addition reactions.<sup>18,19</sup>

(3) We are interested in understanding how Marcus intrinsic barriers to chemical reactions, and the changes in these barriers with changing reactant structure, influence structure–reactivity effects on carbocation–nucleophile addition reactions.<sup>20–24</sup> However, reports in the chemical literature of the determination of these barriers are rare.<sup>24</sup> The kinetic and thermodynamic parameters for addition of halide and acetate ions to **1** allow for determination of the Marcus intrinsic reaction barriers, and an analysis of the relationship between these intrinsic barriers and the effect of changing electrophile reactivity on electrophile selectivity toward addition of nucleophilic reagents.<sup>18,19</sup>

(4) A thorough characterization of the reactivity of quinone methides toward nucleophile addition is one part of the broader description of these compounds required to explain the relationship between their chemical reactivity and their roles in biology.

## Experimental Section

**Materials.** Inorganic salts and organic chemicals were reagent grade from commercial sources and were used without further purification unless noted otherwise. Amine nucleophiles were purchased in the free base form, except for hydroxylamine, which was purchased as  $(\text{NH}_3\text{-OH})_2\text{SO}_4$  and converted to the basic form using sodium hydroxide. HPLC-grade methanol was used for all HPLC analyses. Water for kinetic studies and HPLC analyses was distilled and passed through a Milli-Q water purification system.

4-MeOC<sub>6</sub>H<sub>4</sub>C(CF<sub>3</sub>)<sub>2</sub>OTs (**Me-1-OTs**) was prepared by a published procedure.<sup>25</sup> The quinone methide **1** was generated for use in kinetic and product studies by making a large (25–150-fold) dilution of **Me-1-OTs** (0.15 M – 0.50 M in acetonitrile) into 2/1 (v/v) trifluoroethanol/water to give a final concentration of **Me-1-OTs** that ranged from 1 to 20 mM, depending upon the experiment. A 30% yield of **1** forms in this solvent during a 10 min reaction time.<sup>15</sup> These solutions of **1** in 2/1 (v/v) trifluoroethanol/water were used in kinetic experiments within 4 h of preparation, during which time there was less than 20% conversion of **1** to the corresponding solvent adducts. The concentration of **1** was determined spectrophotometrically at 283 nm using an extinction coefficient of 36 000 M<sup>-1</sup> cm<sup>-1</sup>.<sup>15</sup>

Stock solutions of sodium sulfite and hydrogen peroxide were prepared daily, and their concentrations were determined immediately after their use in a kinetic experiment by titration with starch iodine and KMnO<sub>4</sub>,<sup>26a</sup> respectively. The concentrations of thiols were determined before and after each kinetic run using 5,5'-dithiobis(2-nitrobenzoic acid).<sup>26b</sup> In cases where the thiol concentration was observed to decrease ( $\leq 7\%$ ) during the course of the kinetic run, the concentration during the kinetic run was obtained by averaging the initial and final thiol concentrations.

**pH Measurements and Buffers.** The pH measurements were performed at 25 °C using a combination electrode in which the salt bridge filling solution was replaced by 5 M lithium trichloroacetate.<sup>27</sup> The pH was determined at the end of reactions monitored by conventional UV spectroscopy. It was not possible to measure the final pH of reaction mixtures in the stopped-flow experiments. In these cases, the pH was determined for control solutions that were prepared to be identical to the corresponding solutions from the stopped-flow experiments.

In studies of the reactions of ethylamine (pH 10–11), glycylglycine, (pH 7.6–8.6), and trifluoroethylamine (pH 5.2–6.2) with **1**, the nucleophile also served to buffer the reaction solution. Constant pH was maintained in studies of other nucleophiles by use of the appropriate buffer (0.01–0.05 M): dichloroacetate, pH  $\leq 2.5$ ; chloroacetate, pH 2.7–3.5; methoxyacetate, pH 3–4.2; acetate, pH 4.2–5.3; 2-(*N*-morpholino)ethanesulfonic acid (MES), pH 6–7; 3-(*N*-morpholino)propanesulfonic acid (MOPS), pH 7.5–8; *N*-tris(hydroxymethyl)methyl-3-aminopropanesulfonic acid (TAPS), pH 8–9; 3-(cyclohexylamino)-1-propanesulfonic acid (CAPS), pH 9.5–10.5.

**Product Studies.** Aqueous solutions ( $I = 1.0$ , NaClO<sub>4</sub>) at 25 °C containing **1** and **H-1-Br** or **H-1-I** at chemical equilibrium were prepared by adding measured amounts of HClO<sub>4</sub> and sodium bromide or sodium iodide to solutions that contain a fixed concentration (ca. 10<sup>-5</sup> M) of **1** and monitoring the approach to an equilibrium mixture of **1** and **H-1-Nu** at 283 nm.<sup>16</sup> The ratio  $[\text{H-1-Nu}]_{\text{eq}}/[\text{1}]_{\text{eq}}$  at equilibrium was determined from eq 1, where  $A_0$  is the absorbance of a solution that contains only **1**,  $A_{\text{eq}}$  is the absorbance observed for solutions that contain an equilibrium mixture of **1** and **H-1-Nu**, and  $A_{\text{min}}$  is the limiting minimum absorbance observed for a solution that contains, essentially, only **H-1-Nu**, determined for the reaction of **1** in the presence of high concentrations of H<sup>+</sup> and Nu<sup>-</sup>.

(18) Ritchie, C. D. *Can. J. Chem.* **1986**, *64*, 2239–2250.

(19) Ritchie, C. D. *Acc. Chem. Res.* **1972**, *5*, 348–354.

(20) Richard, J. P.; Amyes, T. L.; Vontor, T. *J. Am. Chem. Soc.* **1992**, *114*, 5626–5634.

(21) Richard, J. P.; Amyes, T. L.; Jagannadham, V.; Lee, Y.-G.; Rice, D. J. *J. Am. Chem. Soc.* **1995**, *117*, 5198–5205.

(22) Richard, J. P. *Tetrahedron* **1995**, *51*, 1535–1573.

(23) Richard, J. P.; Amyes, T. L.; Williams, K. B. *Pure Appl. Chem.* **1998**, *70*, 2007–2014.

(24) Richard, J. P.; Williams, K. B.; Amyes, T. L. *J. Am. Chem. Soc.* **1999**, *121*, 8403–8404.

(25) Allen, A. D.; Kanagasabapathy, V. M.; Tidwell, T. T. *J. Am. Chem. Soc.* **1986**, *108*, 3470–3474.

(26) (a) Kolthoff, I. M.; Belcher, R.; Stenger, V. A.; Matsuma, G. In *Volumetric Analysis*; Interscience Publishers Ltd.: London, 1957; Vol. III. (b) Ellman, G. L. *Arch. Biochem. Biophys.* **1959**, *82*, 70–77.

(27) Herschlag, D.; Jencks, W. P. *J. Am. Chem. Soc.* **1986**, *108*, 7938–46. Washabaugh, M. W.; Jencks, W. P. *J. Am. Chem. Soc.* **1989**, *111*, 674–683.

$$\frac{[\mathbf{H-1-Nu}]_{\text{eq}}}{[\mathbf{1}]_{\text{eq}}} = \frac{A_o - A_{\text{eq}}}{A_{\text{eq}} - A_{\text{min}}} \quad (1)$$

HPLC product studies were carried out in water at 25 °C and  $I = 1.0$  ( $\text{NaClO}_4$ ). Reactions were initiated by making a 100-fold dilution of a solution of **1** to give a final concentration of  $(0.2\text{--}2.0) \times 10^{-4}$  M in an aqueous solution that contains the same volume (2.6%) of trifluoroethanol that was present in the stopped-flow experiments.

**HPLC Analyses.** The products of the reactions of acetate, azide, and propanethiolate anions with **1** were separated by HPLC using procedures described previously,<sup>16,28,29</sup> except that peak detection was by a Waters 996 diode array detector. Substrate and products were detected at 268 nm, which is  $\lambda_{\text{max}}$  for **H-1-OH**.<sup>15</sup> 4-MeOC<sub>6</sub>H<sub>4</sub>C(CF<sub>3</sub>)<sub>2</sub>-OH (**Me-1-OH**), which is formed in ca. 70% yield during the initial generation of **1** from **Me-1-OTs**,<sup>15</sup> was used as an internal standard to correct for small variations in the injection volume. Normalized HPLC peak areas were reproducible to better than  $\pm 10\%$ . Ratios of product yields,  $[\mathbf{H-1-OAc}]/[\mathbf{H-1-OH}]$ , were calculated using eq 2, where  $A_1/A_2$  and  $\epsilon_2/\epsilon_1 = 1.0$  are the ratios of the HPLC peak areas and the molar extinction coefficients at 268 nm, respectively, for the two products. The value of  $\epsilon_2/\epsilon_1 = 1.0$  is assumed, because it has been shown in earlier work that the extinction coefficients of 1-(4-methoxyphenyl)-2,2,2-trifluoroethyl alcohol and 1-(4-methoxyphenyl)-2,2,2-trifluoroethyl acetates are identical at  $\lambda_{\text{max}}$  for the alcohol.<sup>20</sup>

$$[P]_1/[P]_2 = (A_1/A_2)(\epsilon_2/\epsilon_1) \quad (2)$$

**Kinetic Studies.** All kinetic studies were carried out at 25 °C and  $I = 1.0$  ( $\text{NaClO}_4$ ). Reactions in the presence of nucleophilic reagents employed at least a 10-fold excess of nucleophile over **1**. Reactions of **1** with halftimes of less than 5 s were monitored by following the decrease in absorbance at 283 nm using the SX17.MV stopped-flow device from Applied Photophysics. The aqueous solution and a solution of **1** in 2/1 (v/v) trifluoroethanol/water were mixed in a ratio of 25:1 to give a final aqueous reaction mixture containing 2.6% trifluoroethanol and  $1 \times 10^{-5}$  M **1**. First-order rate constants,  $k_{\text{obsd}}$ , were obtained from the fit of the absorbance data to a single-exponential function and were reproducible to  $\pm 5\%$ . The slower reactions of **1** were monitored using a conventional UV spectrophotometer and were initiated by making a 100-fold dilution of **1** to give a final concentration of  $1 \times 10^{-5}$  M **1** in an aqueous solution that contains the same volume (2.6%) of trifluoroethanol that was present in the stopped-flow experiments. First-order rate constants,  $k_{\text{obsd}}$ , were calculated from the slopes of linear semi-logarithmic plots of reaction progress against time and were reproducible to  $\pm 5\%$ .

$$\text{pH} = \text{p}K_a - \log \frac{[\text{NuH}]}{[\text{Nu}]} \quad (3)$$

$$\frac{[\text{NuH}]}{[\text{Nu}]} = \left( \frac{A_{\text{Nu}} - A_{\text{obsd}}}{A_{\text{obsd}} - A_{\text{NuH}}} \right) \quad (4)$$

The second-order rate constants ( $k_{\text{Nu}}_{\text{obsd}}$  ( $\text{M}^{-1} \text{s}^{-1}$ )) for the reaction of nucleophiles with **1** were determined as the least-squares slopes of linear plots of  $k_{\text{obsd}}$  against the total concentration of the nucleophile. The nonlinear least-squares fit to eq 7 of the pH-rate profile for ( $k_{\text{Nu}}_{\text{obsd}}$ ) for the reaction of  $\text{SO}_3^{2-}$  (see Results) was obtained using SigmaPlot from Jandel Scientific.

**Determination and Estimation of Acidity Constants.** Values of ( $\text{p}K_a$ )<sub>HNu</sub> for the conjugate acids of nucleophilic reagents at 25 °C and  $I = 1.0$  ( $\text{NaClO}_4$ ) were determined from the solution pH and the concentration ratios  $[\text{NuH}]/[\text{Nu}]$  according to eq 3, using data at 20–80% protonation of the nucleophile. Except for ethylamine, buffered amine solutions of known  $[\text{RNH}_3^+]/[\text{RNH}_2]$  were prepared by mixing solutions containing known concentrations of perchloric acid and  $\text{RNH}_2$ . The  $\text{p}K_a$  of ethylamine was determined by titration of a solution of

$\text{RNH}_2$  at  $I = 1.0$  ( $\text{NaClO}_4$ ), with correction of the values of the concentration ratio  $[\text{RNH}_3^+]/[\text{RNH}_2]$  for the concentration of hydroxide ion calculated from the pH. Values of the concentration ratio  $[\text{NuH}]/[\text{Nu}]$  for a number of other nucleophiles were determined spectrophotometrically according to eq 4, where  $A_{\text{obsd}}$  is the absorbance of the test solution and  $A_{\text{Nu}}$  and  $A_{\text{Hnu}}$  are the absorbance values of the solution when essentially all of the nucleophile is present in the basic and acidic forms, respectively. The extent of protonation of propanethiolate ion ( $0.1\text{--}0.2$  mM,  $\epsilon_{\text{RS}} > \epsilon_{\text{RSH}}$ ) and peroxide ion ( $0.02$  M,  $\epsilon_{\text{HOO}} > \epsilon_{\text{HOOH}}$ ) was determined at 238 and 260 nm, respectively, which are  $\lambda_{\text{max}}$  for the nucleophilic anions. The extent of protonation of azide ion ( $20$  mM,  $\epsilon_{\text{HN}_3} > \epsilon_{\text{N}_3}$ ) was determined at  $\lambda_{\text{max}}$  for  $\text{HN}_3$  (260 nm).

Values of ( $\text{p}K_a$ )<sub>ArOH</sub> for the phenolic oxygen of **H-1-Nu** were estimated using eq 5, where ( $\text{p}K_a$ )<sub>PhOH</sub> = 10.0 for phenol,<sup>30</sup>  $\rho = 2.2$  is the Hammett reaction constant for ionization of substituted phenols in water,<sup>31</sup> and  $\sigma_{\text{eff}}$  is the effective Hammett substituent constant for  $p\text{-C}(\text{CF}_3)_2\text{Nu}$  estimated using eq 6. Equation 6 was derived assuming additivity of the polar Hammett substituent constants<sup>31</sup> for the groups attached to the benzylic carbon ( $\sigma_p$  for  $\text{CF}_3$  and  $\sigma_n$  for Nu), with an attenuation factor of 0.40 for the carbon that separates these groups from the aromatic ring.<sup>32</sup> This gives  $\sigma_{\text{eff}} = 0.54$  for  $\text{C}(\text{CF}_3)_2\text{Br}$  and  $\sigma_{\text{eff}} = 0.55$  for  $\text{C}(\text{CF}_3)_2\text{I}$ , which were substituted into eq 5 to give ( $\text{p}K_a$ )<sub>ArOH</sub> = 8.8 for both **H-1-Br** and **H-1-I**.

$$(\text{p}K_a)_{\text{ArOH}} = (\text{p}K_a)_{\text{PhOH}} - \rho\sigma_{\text{eff}} \quad (5)$$

$$\sigma_{\text{eff}} = 0.40(2\sigma_{\text{CF}_3} + \sigma_{\text{Nu}}) \quad (6)$$

## Results

By contrast with our previous studies of nucleophile addition to **1** in 50/50 (v/v) trifluoroethanol/water,<sup>16</sup> an aqueous solvent was used in this work, to avoid protonation of basic nucleophiles by trifluoroethanol. A value of  $k_s = 6.4 \times 10^{-4} \text{ s}^{-1}$  for the reaction of **1** with solvent water at 25 °C and  $I = 1.0$  ( $\text{NaClO}_4$ ) was determined by following the decrease in absorbance due to **1** at 283 nm. The products of nucleophilic addition of azide and propanethiolate ions to **1** were detected by HPLC analysis, and it was shown for these nucleophiles that conversion of **1** to the nucleophile adduct is essentially quantitative when  $[\text{Nu}^-] \geq 1$  mM.

First-order rate constants ( $k_{\text{obsd}}$  ( $\text{s}^{-1}$ )) for the disappearance of **1** in the presence of increasing concentrations of nucleophiles in water at 25 °C and  $I = 1.0$  ( $\text{NaClO}_4$ ) were determined by monitoring the decrease in absorbance of **1** at 283 nm, either by conventional or stopped-flow spectrophotometry. Observed second-order rate constants ( $k_{\text{Nu}}_{\text{obsd}}$  ( $\text{M}^{-1} \text{s}^{-1}$ )) for the reactions of  $\text{CH}_3\text{CH}_2\text{CH}_2\text{S}^-$ ,  $\text{HOO}^-$ ,  $\text{SO}_3^{2-}$ ,  $\text{N}_3^-$ , ethylamine, trifluoroethylamine, glycylglycine, and hydroxylamine with **1** were determined as the slopes of linear plots of  $k_{\text{obsd}}$  ( $\text{s}^{-1}$ ) against the total concentration of the acidic and basic forms of the nucleophilic reagent and are reported in Table S1 of the Supporting Information.

Figure 1 shows pH-rate profiles of the observed second-order rate constants ( $k_{\text{Nu}}_{\text{obsd}}$ ) for the reaction of a variety of neutral amines and anionic nucleophiles with **1**. These correlations have slopes of 1.0 at  $\text{pH} \ll (\text{p}K_a)_{\text{NuH}}$  (Scheme 3) and show a downward break, centered at  $(\text{p}K_a)_{\text{NuH}}$ , to a slope of zero in cases where it was possible to obtain values of ( $k_{\text{Nu}}_{\text{obsd}}$ ) at  $\text{pH} \gg (\text{p}K_a)_{\text{NuH}}$ . Table 1 reports the following: (a) values of  $k_{\text{Nu}}$

(30) Jencks, W. P.; Regenstein, J. In *Handbook of Biochemistry and Molecular Biology, Physical and Chemical Data*, 3rd ed.; Fasman, G. D., Ed.; CRC Press: Cleveland, OH, 1976; Vol. 1; pp 305–351.

(31) Hine, J. In *Structural Effects on Equilibria in Organic Chemistry*; Wiley: New York, 1975.

(32) Calculated as the average of the ratios of values of  $\sigma_p$  for  $p\text{-CH}_3\text{I}$ ,  $p\text{-CH}_2\text{Br}$ , and  $p\text{-CH}_2\text{Cl}$  substituents and the corresponding values of  $\sigma_n$  for  $p\text{-I}$ ,  $p\text{-Br}$ , and  $p\text{-Cl}$  substituents.<sup>31</sup>

(28) Richard, J. P.; Rothenberg, M. E.; Jencks, W. P. *J. Am. Chem. Soc.* **1984**, *106*, 1361–1372.

(29) Richard, J. P. *J. Am. Chem. Soc.* **1989**, *111*, 1455–1465.



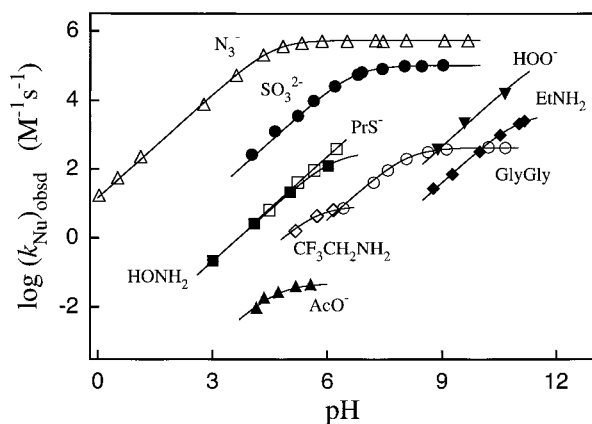


**Figure 1.** pH-rate profiles of the second-order rate constants  $(k_{\text{Nu}})_{\text{obsd}}$  ( $\text{M}^{-1} \text{s}^{-1}$ ) for the addition of neutral and anionic nucleophiles to the quinone methide **1** in water at 25 °C and  $I = 1.0$  ( $\text{NaClO}_4$ ). The lines through the data show the fits to eq 7 (see text).

( $\text{M}^{-1} \text{s}^{-1}$ , Scheme 3) for the reaction of azide ion, sulfite dianion, and glycylglycine with **1**, determined as the average of the values of  $(k_{\text{Nu}})_{\text{obsd}}$  at high pH where >95% of the reagent is present in the basic form (Figure 1); (b) values of  $k_{\text{Nu}}$  for the reaction of  $\text{CH}_3\text{CH}_2\text{CH}_2\text{S}^-$ ,  $\text{HOO}^-$ , ethylamine, trifluoroethylamine, and hydroxylamine with **1**, determined as the average of the values of  $(k_{\text{Nu}})_{\text{obsd}}/f_{\text{Nu}}$ , where  $f_{\text{Nu}}$  is fraction of the nucleophilic reagent present in the basic form. Unless noted otherwise, the uncertainty in the values of  $k_{\text{Nu}}$ , estimated from the range of the values of  $k_{\text{Nu}}$  determined at different pH values, is  $\pm 10\%$ .

$$(k_{\text{Nu}})_{\text{obsd}} = \frac{k_{\text{Nu}}(K_{\text{a}})_{\text{NuH}}}{(K_{\text{a}})_{\text{NuH}} + a_{\text{H}}} \quad (7)$$

The solid lines through the data in Figure 1 were calculated using eq 7 derived for Scheme 3 and the values of  $k_{\text{Nu}}$  ( $\text{M}^{-1} \text{s}^{-1}$ ) and the  $\text{p}K_{\text{a}}$  of the nucleophile given in Table 1. The  $\text{p}K_{\text{a}}$ 's were determined by direct titration of the nucleophile under our experimental conditions (see the Experimental Section) except for  $(\text{p}K_{\text{a}})_{\text{HNu}} = 6.7$  for  $\text{HSO}_3^-$ , which was obtained from the nonlinear least-squares fit of the experimental data to eq 7. This is in good agreement with  $\text{p}K_{\text{a}} = 6.6$  for  $\text{HSO}_3^-$  determined at  $I = 1.0$  ( $\text{KCl}$ ).<sup>33</sup> The good fits of the experimental data to eq 7 derived for the mechanism in Scheme 3 show that (a) there are no detectable reactions of the protonated nucleophiles with **1** in the pH range of these experiments and (b) there is no detectable reaction of the sulfate ion that was present in the solutions of hydroxylamine prepared from  $(\text{NH}_3\text{OH})_2\text{SO}_4$ .

The disappearance of **1** in the presence of  $\text{CH}_3\text{CO}_2^-$  followed good first-order kinetics when  $[\text{1}] \leq 5 \times 10^{-5} \text{ M}$ , but deviations were observed at  $[\text{1}] > 5 \times 10^{-5} \text{ M}$ . Similarly, only **H-1-OH** and **H-1-OAc** were observed by HPLC analysis of the products of the reaction of **1** with acetate ion when  $[\text{1}] \leq 2.0 \times 10^{-5} \text{ M}$ , but an additional product with a relatively long HPLC retention time was detected for this reaction at  $[\text{1}] > 2.0 \times 10^{-5} \text{ M}$ . The fractional yield of this product increased as the pH was increased. These data are consistent with the conclusion that the additional product forms by addition of the phenoxide anion **1-OAc** to a second molecule of **1** to give a dimeric product **H-1-1-OAc**. However, this product was not further characterized.

We have restricted our analysis of kinetic and product data for the reactions of acetate ion to concentrations of **1** ( $\leq 2.0 \times 10^{-5} \text{ M}$ ) where the reaction is cleanly first order in **1** and **H-1-OH** and **H-1-OAc** are the only detectable products. Observed second-order rate constants,  $(k_{\text{AcO}})_{\text{obsd}}$  ( $\text{M}^{-1} \text{s}^{-1}$ ), for the reactions of **1** in acetate buffers were determined as the slopes of linear plots of  $k_{\text{obsd}}$  against the total concentration of acetate buffer. A value of  $(k_{\text{Nu}} + k_{\text{B}}) = 0.049 \text{ M}^{-1} \text{s}^{-1}$  (Scheme 4) was calculated as the average of the values  $(k_{\text{AcO}})_{\text{obsd}}/f_{\text{AcO}}$  at five different values of  $f_{\text{AcO}}$  between 0.2 and 0.9, where  $f_{\text{AcO}}$  is the fraction of buffer present as acetate anion. The relative contributions of the reaction of acetate ion to give the nucleophile ( $k_{\text{Nu}}$ , Scheme 4) and the solvent adduct ( $k_{\text{B}}$ ) were determined from the effect of increasing concentrations of acetate ion on the product ratio  $[\text{H-1-OH}]/[\text{H-1-OAc}]$  for reactions at  $[\text{1}] = 1.6 \times 10^{-5} \text{ M}$  (Figure 2). The line through the data in Figure 2 shows the linear fit of the product data to eq 8, and the y-intercept gives  $k_{\text{B}}/k_{\text{Nu}} = 0.029$  (Scheme 4). This corresponds to a limiting yield of ca. 3% of the solvent adduct **H-1-OH** for the reaction of **1** in the presence of high concentrations of acetate ion. The value of  $k_{\text{B}}/k_{\text{Nu}} = 0.029$  was combined with  $(k_{\text{Nu}} + k_{\text{B}}) = 0.049 \text{ M}^{-1} \text{s}^{-1}$  to give  $k_{\text{Nu}} = 0.048 \text{ M}^{-1} \text{s}^{-1}$  for nucleophilic addition of acetate ion to **1** and  $k_{\text{B}} = 0.001 \text{ M}^{-1} \text{s}^{-1}$  for reaction of acetate ion as a general base catalyst of the addition of solvent water.

$$\frac{[\text{H-1-OH}]}{[\text{H-1-OAc}]} = \frac{k_{\text{B}}}{k_{\text{Nu}}} + \frac{k_{\text{s}}}{k_{\text{Nu}}[\text{AcO}^-]} \quad (8)$$

$$\frac{[\text{H-1-Nu}]_{\text{eq}}}{[\text{1}]_{\text{eq}}} = [\text{H}^+][\text{Nu}^-]K_{\text{add}}^{\text{OH}} \quad (9)$$

$$(k_{\text{Nu}})_{\text{obsd}} = k_{\text{Nu}} + k_{\text{HNu}}[\text{H}^+] \quad (10)$$

The reaction of **1** in acidic solutions containing  $\text{Br}^-$  or  $\text{I}^-$  to give **H-1-Br** or **H-1-I** (Scheme 5) in water at 25 °C and  $I = 1.0$  ( $\text{NaClO}_4$ ) was monitored at 283 nm. These reactions proceed essentially quantitatively to the nucleophile adduct when  $[\text{H}^+][\text{Nu}^-]$  is large, but at smaller values of  $[\text{H}^+][\text{Nu}^-]$  equilibrium mixtures of **1** and **H-1-Br** or **H-1-I** are obtained. Figure 3 shows the linear dependence of  $[\text{H-1-Nu}]_{\text{eq}}/[\text{1}]_{\text{eq}}$  at chemical equilibrium on  $[\text{H}^+][\text{Nu}^-]$ , according to eq 9. The slopes of these plots give the equilibrium constants  $K_{\text{add}}^{\text{OH}} = 1.5 \times 10^4$  and  $1.5 \times 10^5 \text{ M}^{-2}$  for the addition of  $\text{HBr}$  and  $\text{HI}$ , respectively, to **1** to give **H-1-Nu**.

First-order rate constants,  $k_{\text{obsd}}$  ( $\text{s}^{-1}$ ), for the essentially complete reaction of **1** with halide ions in the presence of hydronium ion to give **H-1-Nu** were determined in water at 25 °C and  $I = 1.0$  ( $\text{NaClO}_4$ ), and observed second-order rate constants  $(k_{\text{Nu}})_{\text{obsd}}$  ( $\text{M}^{-1} \text{s}^{-1}$ ) for these reactions were determined as the slopes of plots of  $k_{\text{obsd}}$  against  $[\text{Nu}^-]$ . Figure 4 shows the small increases in  $(k_{\text{Nu}})_{\text{obsd}}$  with increasing concentrations of  $\text{HClO}_4$  for the reactions of iodide, bromide, and chloride ions with **1**. The data were fit to eq 10, derived for the mechanism in Scheme 5; the intercepts of these plots give  $k_{\text{Nu}}$  ( $\text{M}^{-1} \text{s}^{-1}$ , Table 1) for direct addition of the halide ion to **1**, and the slopes give  $k_{\text{HI}} = 110 \text{ M}^{-2} \text{s}^{-1}$ ,  $k_{\text{HBr}} = 7.4 \text{ M}^{-2} \text{s}^{-1}$ , and  $k_{\text{HCl}} = 1.2 \text{ M}^{-2} \text{s}^{-1}$  as the third-order rate constants for the specific-acid-catalyzed reactions of iodide, bromide, and chloride ions with **1**, respectively.

## Discussion

The observed second-order rate constants for nucleophile addition to **1** (Figure 1) are directly proportional to the fraction

(33) Young, P. R.; Jencks, W. P. *J. Am. Chem. Soc.* **1977**, *99*, 8238–8248.



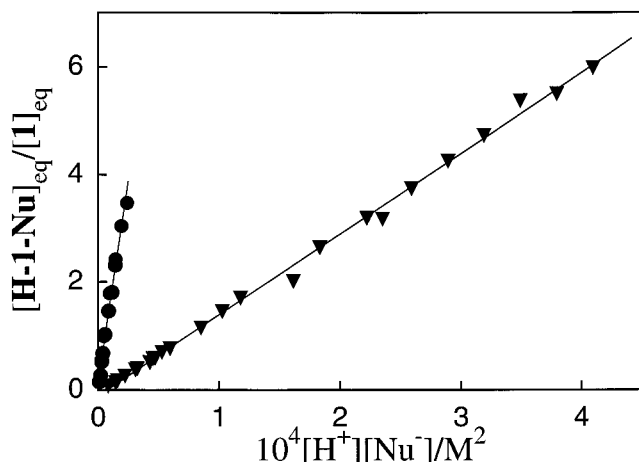


**Figure 3.** Dependence of the ratio of the concentrations of **H-1-Nu** and **1** at chemical equilibrium on the product of concentrations  $[H^+][Nu^-]$  in water at 25 °C and  $I = 1.0$  ( $NaClO_4$ ): ●, data for addition of HI; ▼, data for addition of HBr.

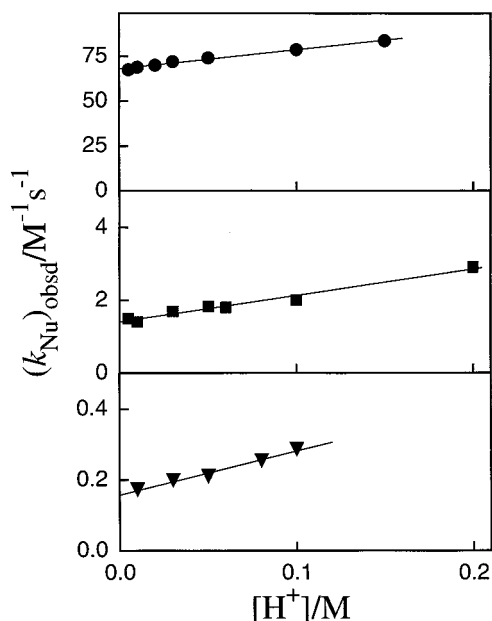


**Figure 4.** Dependence of the second-order rate constant  $(k_{Nu})_{obsd}$  ( $M^{-1} s^{-1}$ ) for the addition of halide ions to **1** on the concentration of hydronium ion in water at 25 °C and  $I = 1.0$  ( $NaClO_4$ ): ●, acid-catalyzed addition of iodide ion; ■, acid-catalyzed addition of bromide ion; ▼, acid-catalyzed addition of chloride ion.

**Reactions of Halide Ions.** Two pathways were observed for the reaction of halide ions with **1**. The dominant reaction is the direct addition of the halide ion to **1** ( $k_{Nu}$ , Scheme 5) to give the phenoxide anion **1-Nu**, which is in rapid equilibrium with **H-1-Nu**. The specific-acid-catalyzed addition of halide ions to give **H-1-Nu** directly is also observed (Figure 4) in strongly acidic solutions ( $k_{H-Nu}$ , Scheme 5).

The values of  $k_{Nu}$  ( $M^{-1} s^{-1}$ , Table 1) and  $k_{H-Nu}$  ( $M^{-2} s^{-1}$ , Results) for the uncatalyzed and specific-acid-catalyzed addition of halide ions to **1** in water at 25 °C ( $I = 1.0$ ,  $NaClO_4$ ) are 6–8-fold and <3-fold larger, respectively, than the correspond-

ing rate constants for these reactions in 50/50 (v/v) trifluoroethanol/water.<sup>16</sup> The larger values of  $k_{Nu}$  in water than in trifluoroethanol/water are probably due to stabilization of the halide ion by hydrogen bonding to the relatively acidic solvent trifluoroethanol. The smaller effect of this change in solvent on the values of  $k_{H-Nu}$  is consistent with a compensating greater activity of the proton in trifluoroethanol/water than in water.

Table 2 gives the values of  $K_{add}^{OH}$  ( $M^{-2}$ ), the overall equilibrium constant for the addition of HBr and HI to **1** to give **H-1-Nu**, determined directly as described in the Experimental Section (Scheme 5). These experimental equilibrium constants and the values of  $k_{Nu}$  ( $M^{-1} s^{-1}$ , Table 1) for halide ions were used to calculate the following rate and equilibrium constants and intrinsic reaction barriers reported in Table 2:

(1) Values of  $K_{add}$  ( $M^{-1}$ ) for addition of bromide and iodide ions to **1** to give **1-Br** and **1-I** were calculated using the relationship  $K_{add} = K_{add}^{OH}(K_a)_{ArOH}$  (Scheme 5), where  $(K_a)_{ArOH}$  is the estimated acidity constant for ionization of **H-1-Nu** to give **1-Nu** (see the Experimental Section).

(2) Values of  $k_{solv}$  ( $s^{-1}$ ) for the expulsion of halide ions from **1-Br** and **1-I** to give **1** were calculated from the values of  $K_{add}$  using the relationship  $k_{solv} = k_{Nu}/K_{add}$  (Scheme 5).

(3) Values of  $k_{solv}$  ( $s^{-1}$ ) for the expulsion of chloride and acetate ions from **1-Cl** and **1-OAc** to give **1** were estimated from the value of  $k_{solv}$  for **1-Br** and  $(k_{solv})_{Br}/(k_{solv})_{Cl} = 14$  for the ratio of rate constants for the  $D_N + A_N$  ( $S_N1$ ) solvolysis of 1-phenylethyl bromide and chloride<sup>36</sup> and  $(k_{solv})_{Br}/(k_{solv})_{AcO} = 10^7$  for the corresponding ratio for solvolysis of 1-phenylethyl bromide and acetate.<sup>36,37</sup>

(4) Values of  $K_{add}$  ( $M^{-1}$ ) for the addition of chloride and acetate ions to **1** to give **1-Cl** and **1-OAc** were calculated from the values of  $k_{solv}$  using the relationship  $K_{add} = k_{Nu}/k_{solv}$ .

$$\log k_{Nu} = \frac{1}{1.36} \left[ 17.44 - \Lambda \left( 1 - \frac{1.36 \log K_{add}}{4\Lambda} \right)^2 \right] \quad (11)$$

(5) The Marcus intrinsic barriers  $\Lambda$  (kcal/mol) for the thermoneutral addition of chloride, bromide, iodide and acetate ions to **1** to give the respective nucleophile adducts **1-Nu** were calculated from the rate constants  $k_{Nu}$  and equilibrium constants  $K_{add}$  using the Marcus equation (eq 11, derived at 298 K).

Table 2 gives the corresponding values of  $K_{add}$  ( $M^{-1}$ ),  $k_{Nu}$  ( $M^{-1} s^{-1}$ ), and  $k_{solv}$  ( $s^{-1}$ ) for addition of chloride, bromide, and acetate ions to the triphenylmethyl carbocation (**H<sub>3</sub>-2**) that were taken from earlier work by McClelland and co-workers.<sup>38</sup> The rate constants  $k_{Nu}$  and equilibrium constants  $K_{add}$  were substituted into eq 11 to give the intrinsic barriers  $\Lambda$  (kcal/mol) for addition of these nucleophiles to **H<sub>3</sub>-2** (Table 2).

**Structure and Reactivity of Quinone Methides.** While **1** is formally neutral, the large stabilization associated with formation of a  $6\pi$  aromatic system favors a significant contribution of the zwitterionic valence bond structure of the 4- $O^-$ -substituted benzyl carbocation. The following experimental observations show that, by the criterion of its chemical reactivity toward nucleophilic reagents, **1** is a member of the class of

(36) Noyce, D. S.; Virgilio, J. A. *J. Org. Chem.* **1972**, *37*, 2643–2647.

(37) We have chosen to cite the extensive set of data for solvolysis reactions of ring-substituted 1-phenylethyl derivatives. However, these relative leaving group abilities are not strongly substrate dependent so that the uncertainty in these ratios will not affect the interpretation of these results. For example, values of  $(k_{solv})_{Br}/(k_{solv})_{Cl} = 27$  and  $(k_{solv})_{Br}/(k_{solv})_{AcO} = 10^8$  have been estimated for solvolysis reactions of triphenylmethyl derivatives.<sup>38</sup>

(38) McClelland, R. A.; Banait, N.; Steenken, S. *J. Am. Chem. Soc.* **1986**, *108*, 7023–7027.

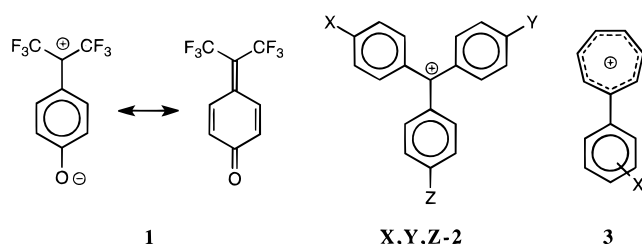
(35) General base catalysis by tertiary amines has been reported for addition of water to **X**, **Y**, **Z-2** in cases where the quaternary ammonium ion adduct is unstable.<sup>39,70,71</sup> However, this reaction is much slower than direct addition of amine nucleophiles. For example, values of  $k_B = 0.036 M^{-1} s^{-1}$  and  $k_{Nu} = 7.4 M^{-1} s^{-1}$ , respectively, were determined for quinuclidine-catalyzed addition of water<sup>71</sup> and direct addition of *n*-propylamine<sup>72</sup> to malachite green, **(Me<sub>2</sub>N)<sub>2</sub>, H-2**.

**Table 2.** Rate and Equilibrium Constants and Intrinsic Reaction Barriers for the Addition of Nucleophiles to the Quinone Methide **1** and the Triphenylmethyl Carbocation **H<sub>3</sub>-2** in Water at 25 °C

nucleophile and electrophile	$k_{\text{Nu}}$ ( $\text{M}^{-1} \text{s}^{-1}$ ) <sup>a</sup>	$K_{\text{add}}^{\text{OH}}$ ( $\text{M}^{-2}$ ) <sup>b</sup>	$K_{\text{add}}$ ( $\text{M}^{-1}$ ) <sup>c</sup>	$k_{\text{solv}}$ ( $\text{s}^{-1}$ ) <sup>d</sup>	$\Delta G^\circ$ (kcal/mol) <sup>e</sup>	$\Delta\Delta G^\circ$ (kcal/mol) <sup>f</sup>	$\Lambda$ (kcal/mol) <sup>g</sup>	$\Delta\Lambda$ (kcal/mol) <sup>h</sup>	anion solvation energy (kcal/mol) <sup>i</sup>
$\text{Cl}^- + \mathbf{1}$	0.16		$\sim 4 \times 10^{-5}$	$\sim 4 \times 10^3$ <sup>j</sup>	6.0		15.4		
$\text{Cl}^- + \mathbf{H}_3\text{-2}$	$2.2 \times 10^6$ <sup>k</sup>		$70$ <sup>k</sup>	$3 \times 10^4$ <sup>k</sup>	-2.5	8.5	10.0	5.4	75
$\text{Br}^- + \mathbf{1}$	1.4	$1.5 \times 10^4$	$2.4 \times 10^{-5}$	$6 \times 10^4$ <sup>j</sup>	6.3		13.9		
$\text{Br}^- + \mathbf{H}_3\text{-2}$	$5 \times 10^6$ <sup>k</sup>		$6$ <sup>k</sup>	$8 \times 10^5$ <sup>k</sup>	-1.1	7.4	8.9	5.0	70
$\text{I}^- + \mathbf{1}$	68	$1.5 \times 10^5$	$2.4 \times 10^{-4}$	$3 \times 10^5$ <sup>j</sup>	4.9		12.4		61
$\text{AcO}^- + \mathbf{1}$	0.048		$\sim 8$	$\sim 0.006$ <sup>j</sup>	-1.2		19.8		
$\text{AcO}^- + \mathbf{H}_3\text{-2}$	$4 \times 10^5$ <sup>k</sup>		$6 \times 10^7$ <sup>k</sup>	$7 \times 10^{-3}$ <sup>k</sup>	-10.6	9.4	14.6	5.2	75

<sup>a</sup> Second-order rate constant for uncatalyzed addition of nucleophile to **1** (Scheme 5, data from Table 1) or **H<sub>3</sub>-2** to give the corresponding nucleophile adduct. <sup>b</sup> Overall equilibrium constants for addition of HNu to **1** to give **H-1-Nu**, determined as described in the Experimental Section (Figure 3 and Scheme 5). <sup>c</sup> Equilibrium constant for addition of the anionic nucleophile to **1** to give **1-Nu** (Scheme 5), see text. <sup>d</sup> First-order rate constant for breakdown of the nucleophile adduct by expulsion of the anionic leaving group (Scheme 5). <sup>e</sup> Gibbs free energy change for addition of the nucleophile to **1** or **H<sub>3</sub>-2**. <sup>f</sup> Difference in the Gibbs free energy changes for addition of the nucleophile to **1** and **H<sub>3</sub>-2**. <sup>g</sup> Marcus intrinsic barrier for addition of the nucleophile to **1** or **H<sub>3</sub>-2** calculated from the values of  $k_{\text{Nu}}$  ( $\text{M}^{-1} \text{s}^{-1}$ ) and  $K_{\text{add}}$  given in this table using eq 11. <sup>h</sup> Difference in the intrinsic barriers  $\Lambda$  for addition of the nucleophile to **1** or **H<sub>3</sub>-2**. <sup>i</sup> The free energy change for transfer of the anion from the gas phase into aqueous solution. Data from ref 52. <sup>j</sup> Calculated from the values of  $K_{\text{add}}$  and  $k_{\text{Nu}}$  using the relationship  $k_{\text{solv}} = k_{\text{Nu}}/K_{\text{add}}$  (Scheme 5). <sup>k</sup> Data from ref 38.

highly resonance-stabilized carbocations, which includes ring-substituted triarylmethyl carbocations (**X,Y,Z-2**) and the aryl triptylium ions (**3**).



(1) The absolute rate constant for addition of solvent water to **1** at 25 °C,  $k_s = 6.4 \times 10^{-4} \text{s}^{-1}$ , lies within the range of rate constants determined for addition of solvent to ring-substituted triarylmethyl carbocations. For example, values of  $k_s = 4.6 \times 10^{-3}$ ,  $2.1 \times 10^{-4}$ , and  $2.0 \times 10^{-5} \text{s}^{-1}$  at 25 °C have been determined for addition of solvent water to **Me<sub>2</sub>N,MeO,H-2**, **(Me<sub>2</sub>N)<sub>2</sub>H-2**, and **(Me<sub>2</sub>N)<sub>3</sub>-2**, respectively.<sup>39</sup>

(2) Rate constants for the addition of nucleophiles to resonance-stabilized carbocations such as **2** and **3** in water show a good fit to the Ritchie  $N_+$  equation (eq 12), where  $N_+$  is a parameter characteristic of nucleophile reactivity.<sup>18,19,40</sup> Figure 5A shows that there is a good linear logarithmic correlation between the rate constants  $k_{\text{Nu}}$  ( $\text{M}^{-1} \text{s}^{-1}$ ) for addition of nucleophiles to **1** and the Ritchie nucleophilicity parameter  $N_+$ . The slope of this correlation is  $s = 0.92 \pm 0.10$ ,<sup>41</sup> which is not significantly different from the value of 1.0 determined for addition of nucleophiles to the resonance-stabilized carbocations **2** and **3**.

$$\log k_{\text{Nu}} = N_+ + \text{constant} \quad (12)$$

(3) There are nearly constant differences between the values of  $\Delta G^\circ$  ( $\Delta G^\circ(\mathbf{1}) - \Delta G^\circ(\mathbf{H}_3\text{-2}) = 8.4 \pm 1.0 \text{kcal/mol}$ ) and of  $\Lambda$

(39) Ritchie, C. D.; Wright, D. J.; Huang, D. S.; Kamego, A. A. *J. Am. Chem. Soc.* **1975**, *97*, 1163–1170.

(40) Ritchie, C. D.; Wright, D. J. *J. Am. Chem. Soc.* **1971**, *93*, 6574–6577.

(41) The value  $k_s = 1.3 \times 10^{-2} \text{s}^{-1}$  for addition of solvent to **1** calculated using a value of  $N_+ = 0$  for solvent is significantly larger than the observed value of  $6.4 \times 10^{-4} \text{s}^{-1}$ . This deviation is another example of a poor correlation of the rate constant for addition of solvent with the Ritchie  $N_+$  equation.<sup>18</sup>

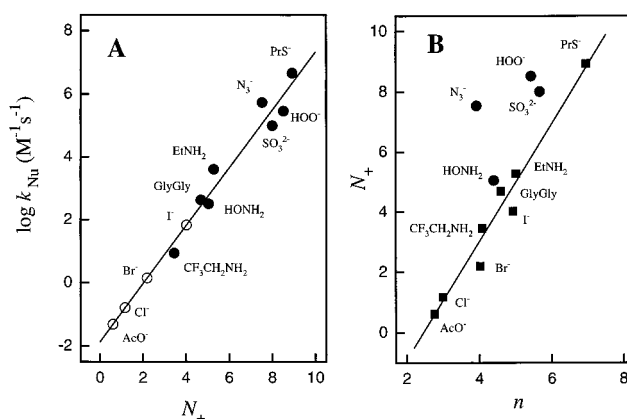


**Figure 5.** (A) Correlation of the second-order rate constants  $k_{\text{Nu}}$  ( $\text{M}^{-1} \text{s}^{-1}$ ) for the addition of nucleophiles to **1** in water at 25 °C and  $I = 1.0$  ( $\text{NaClO}_4$ ) with Ritchie  $N_+$  values (data from Table 1). The solid symbols are the experimental data that were used to obtain the correlation line of slope  $0.92 \pm 0.10$ ; the open symbols are the data for nucleophiles for which values of  $N_+$  have not previously been determined and which are assumed to follow this correlation. (B) Correlation of the values of  $N_+$  for nucleophile addition to trivalent carbon electrophiles with the Swain–Scott  $n$  values for bimolecular nucleophilic substitution at aliphatic carbon (data from Table 1).

( $\Lambda(\mathbf{1}) - \Lambda(\mathbf{H}_3\text{-2}) = 5.2 \pm 0.2 \text{kcal/mol}$ ) for the addition of chloride, bromide, and acetate ions to **1** and **H<sub>3</sub>-2** (Table 2). The ca. 8 kcal/mol more unfavorable change in  $\Delta G^\circ$  for nucleophile addition to **1** than to **H<sub>3</sub>-2** shows that resonance electron donation to the benzylic carbon of **1** is much more stabilizing than the corresponding electron donation from the three phenyl rings at **H<sub>3</sub>-2**. The ca. 5 kcal/mol larger intrinsic barrier for nucleophile addition to **1** is consistent with the notion that the effect of this larger carbocation stabilization by resonance is to make carbocation–nucleophile addition more difficult in both a thermodynamic and a kinetic sense.<sup>22,23,42</sup> The almost constant relative values of  $\Lambda$  and  $\Delta G^\circ$  for the addition of different nucleophiles to **1** and **H<sub>3</sub>-2** is striking and requires that variations in nucleophile structure bring about the same change in both the transition state and product stability for nucleophilic addition to these two electrophiles. This provides

(42) (a) Bernasconi, C. F.; Killion, R. B., Jr. *J. Am. Chem. Soc.* **1988**, *110*, 7506–7512. (b) Bernasconi, C. F.; Ketner, R. J.; Chen, X.; Rappoport, Z. *J. Am. Chem. Soc.* **1998**, *120*, 7461–7468.



good evidence for the development of similar electrophile–nucleophile bonding interactions at these transition states and products.

**Structure–Reactivity Relationships and Intrinsic Barriers.** There is no simple relationship between the rate and equilibrium constants for the addition of nucleophiles to **1** or for addition to the triphenylmethyl carbocation **H<sub>3</sub>-2** (Table 2). For example, nucleophilic addition of acetate ion to **1** is 6.1 kcal/mol more favorable than addition of iodide ion, but the rate constant for addition of iodide ion is 1400-fold larger than that for acetate ion (Table 2). Such breakdowns in rate–equilibrium relationships are a direct consequence of differences in the intrinsic barriers for the two nucleophile addition reactions. Thus, the *larger* rate constants for addition of iodide ion to **1** than for the thermodynamically more favorable addition of acetate ion reflects the 7.4 kcal/mol *smaller* intrinsic barrier for the iodide ion reaction (Table 2). Similarly, the observation of decreasing rate constants  $k_I > k_{Br} > k_{Cl}$  for addition of halide ions to **1**, for reactions that are of *similar thermodynamic driving force*, reflects the increase in the intrinsic reaction barrier along the series  $\Delta_I < \Delta_{Br} < \Delta_{Cl}$  (Table 2). The tendency of *soft* polarizable thiolate anions to show smaller intrinsic barriers than harder nucleophilic amines<sup>42a</sup> and alkoxide anions<sup>42b</sup> toward addition to  $\alpha$ -nitrostilbenes and methoxybenzylidene Meldrum's acid, respectively, has been noted in earlier work.

These data provide another example of how changes in the intrinsic kinetic *ease* of chemical reactions, as measured by changes in their intrinsic reaction barrier, strongly influence observed structure–reactivity relationships.<sup>22,23</sup> They suggest that, in developing rationalizations of structure–reactivity relationships, knowledge of the intrinsic barriers  $\Delta$  is as important as knowledge of the Gibbs free energy changes  $\Delta G^\circ$ , and that the determination of these intrinsic barriers will often be essential for a complete characterization of structure–reactivity relationships.

The principle of nonperfect synchronization provides a useful framework to explain such differences in intrinsic reaction barriers.<sup>43–45</sup> This principle can be understood by imagining, for any thermoneutral reaction, that the absence of a thermodynamic driving force reflects the exact balancing of interactions that tend to destabilize product relative to reactant and interactions that tend to stabilize product relative to reactant. Part or all of the observed barriers to these reactions may then reflect the larger *fractional* expression of product-destabilizing interactions at the transition state, relative to expression of the balancing product-stabilizing interactions or *nonperfect synchronization* in the expression of these interactions. Similarly, changes in the relative magnitude of the expression of different product-stabilizing and product-destabilizing interactions will result in changes in the intrinsic kinetic barrier  $\Delta$ .<sup>43–45</sup>

There are at least two interactions that might account for some or all of the changes in intrinsic barriers with changing nucleophile that are observed for the addition of halide and acetate ions to **1** and **H<sub>3</sub>-2**:

**(1) Solvation of the Reacting Nucleophile.** There is a good correlation between the change in solvation energy for halide ions and the change in intrinsic barrier for addition of halide ions to **1** or **H<sub>3</sub>-2** to form a product at which the stabilizing solvation of the halide ion is largely lost (Table 2).<sup>46</sup> It is useful

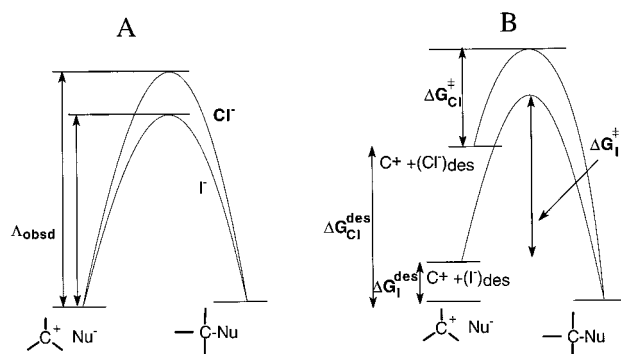


**Figure 6.** Hypothetical reaction coordinate profiles for the addition of iodide and chloride ions to electrophilic trivalent carbon. (A) Profiles for thermoneutral reactions which do not specifically consider desolvation of the nucleophile prior to its reaction. (B) Profiles for formally thermoneutral reactions in which unfavorable desolvation of the nucleophile ( $\Delta G_{Cl}^{des}$  and  $\Delta G_I^{des}$ ) precedes covalent bond formation to the electrophile and the actual reaction barriers for reaction of the desolvated nucleophiles ( $\Delta G_{Cl}^{\ddagger}$  and  $\Delta G_I^{\ddagger}$ ) are significantly smaller than those for reaction of the solvated nucleophiles.

to treat separately the following changes in solvation of the nucleophile that occur for nucleophilic addition reactions:

(a) Cleavage of a hydrogen bond between water and halide ion to free an electron pair to react with an electrophile, which may make a significant contribution to the observed barrier to the nucleophile addition reactions.<sup>47–50</sup> This represents “work” that needs to be done on reactants before bond formation can occur. Figure 6 shows that the relative intrinsic barriers for nucleophile addition may change dramatically depending upon whether the “work” done in nucleophile desolvation is included in the overall change in free energy for the reaction. Different barriers to preequilibrium desolvation for the formally thermoneutral nucleophile additions (Figure 6A) would result in differences in the *chemical driving force* for reactions of the “partly desolvated” nucleophile (Figure 6B). Now, the *true* intrinsic barriers calculated for thermoneutral reactions of these “partly desolvated” halide ions would be smaller than the intrinsic barriers calculated directly from the experimental rate and equilibrium data using eq 11, with the decrease being the largest for the most strongly solvated chloride ion and the smallest for the most weakly solvated iodide ion. The net result is to reduce the *differences* in intrinsic barriers for the reactions of desolvated halide ions, relative to those calculated using the experimental data in Table 2.

(b) All other changes in the 60–80 kcal/mol interaction between solvent and the anionic nucleophile (Table 2) that are lost upon carbocation–nucleophile bond formation. It is possible that the intrinsic barriers for gas-phase carbocation–halide ion addition reactions are similar and that the observed differences in the barriers for these reactions in water (Table 2) are the result of the requirement for a larger fractional loss of reactant-stabilizing halide ion solvation at the transition state relative to the product-stabilizing bond formation to the nucleophile. However, the timing between changes in nucleophile solvation and bond formation to electrophilic carbocations is not well understood.

**(2) Bonding Interactions between the Nucleophile and Electrophile.** There is a good correlation between the increasing

(43) Bernasconi, C. F. *Adv. Phys. Org. Chem.* **1992**, 27, 119–238. Bernasconi, C. F. *Tetrahedron* **1985**, 41, 3219–3234.

(44) Bernasconi, C. F. *Acc. Chem. Res.* **1987**, 20, 301–308.

(45) Bernasconi, C. F. *Acc. Chem. Res.* **1992**, 25, 9–16.

(46) The anion solvation energies were taken from Table 1 in ref 52.

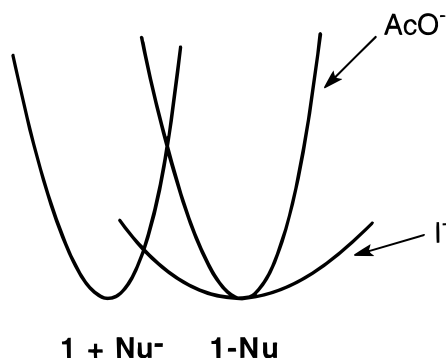
(47) McClelland, R. A.; Kanagasabapathy, V. M.; Banait, N. S.; Steenken, S. *J. Am. Chem. Soc.* **1992**, 114, 1816–1823.

(48) Richard, J. P.; Jencks, W. P. *J. Am. Chem. Soc.* **1984**, 106, 1373–1383.

(49) Richard, J. P. *J. Chem. Soc., Chem. Commun.* **1987**, 1768–1769.

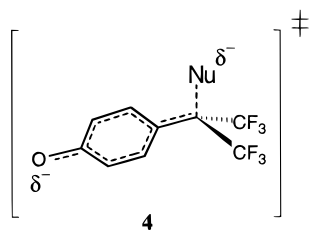
(50) Berg, U.; Jencks, W. P. *J. Am. Chem. Soc.* **1991**, 113, 6997–7002.

Scheme 6



intrinsic reaction barriers for nucleophile addition to **1** (Table 2) and the decreasing  $\alpha$ -deuterium isotope effects  $k_H/k_D$  for bimolecular nucleophile substitution at *N*-(methoxymethyl)-*N,N*-dimethylanilinium ions ( $\text{Nu}^-$ ,  $k_H/k_D$ :  $\text{I}^-$ , 1.18;  $\text{Br}^-$ , 1.16;  $\text{Cl}^-$ , 1.13;  $\text{AcO}^-$ , 1.07).<sup>51a</sup> These isotope effects are consistent with an “open” transition state for the bimolecular substitution reaction of iodide ion, where the hybridization of the  $\alpha$ -carbon is close to that for the free methoxymethyl carbocation, and a change to a transition state with greater bonding to the  $\alpha$ -carbon on moving along the series  $\text{I}^-$ ,  $\text{Br}^-$ ,  $\text{Cl}^-$ ,  $\text{AcO}^-$ . They provide evidence that large “soft” polarizable nucleophiles such as iodide ion can interact from a greater distance to provide electronic overlap with an electron deficient bonding orbital than can “hard” more weakly polarizable nucleophiles such as chloride and acetate ions. A similar trend has been observed for the *inverse*  $\alpha$ -deuterium isotope effects on the addition of halide ions and solvent to diarylmethyl carbocations ( $\text{Nu}^-$ ,  $k_H/k_D$ :  $\text{Br}^-$ , 0.96;  $\text{Cl}^-$ , 0.94;  $\text{H}_2\text{O}$ , 0.88).<sup>51b</sup>

The greater tendency of iodide ion compared with oxygen nucleophiles to form *stabilizing covalent interactions* from a distance may result in a transition state that is “earlier” in the sense that it occurs at a larger carbon–iodine bond distance. This may be represented by the free energy profiles shown in Scheme 6, where cleavage of the bond to iodine at **1-I** occurs along a flatter potential energy surface than that for cleavage of the bond to oxygen at **1-OAc**, due to the (proposed) greater fractional expression of the bonding interactions as the bond to the former leaving group is stretched.



There is also a correlation between the decreasing relative stability of the transition states **4** for the addition of halide ions along the series  $\text{I}^-$ ,  $\text{Br}^-$ ,  $\text{Cl}^-$  ( $\Delta_I < \Delta_{\text{Br}} < \Delta_{\text{Cl}}$ ) and the relative one-electron ionization potentials of halide ions in water,  $I_1 > I_{\text{Br}} > I_{\text{Cl}}$ .<sup>52</sup> The bonds between halide ions and **1** or **H<sub>3</sub>-2** have significant covalent character and involve formal donation of a single electron from the nucleophile to the reacting carbon.<sup>53</sup> It has been suggested that the valence-bond configuration for

homolytic bond cleavage to form radical products makes a significant contribution to the transition state for formal heterolytic bond cleavage and that these transition states have a certain “radical” character.<sup>53</sup> This might account for the observed increase in the stability of transition states for nucleophile addition to **1** with decreasing ionization potentials reflect the increasing stability of this nucleophile radical, and they may be manifested in the transition state for nucleophile addition in proportion to the contribution of the valence-bond configuration for the nucleophile radical to the overall transition state structure.

Different requirements for nucleophile desolvation, or the different ease of one-electron transfer, cannot easily account for the ca. 4.5 kcal/mol smaller intrinsic barrier for the addition of chloride than of acetate ion to **1** or **H<sub>3</sub>-2**, because the solvation energies (Table 2) and one-electron oxidation potentials<sup>52</sup> of these nucleophiles are similar. We do not know the explanation for this difference in intrinsic reaction barriers.

**The Ritchie  $N_+$  Relationship.** The values of  $N_+$  for halide ions have not been determined because of the large kinetic and thermodynamic instability of their adducts to resonance-stabilized carbocations such as **2** and **3**, and only an estimate of  $N_+ < 2.95$  has been reported for acetate ion.<sup>54a</sup> We have obtained values of  $N_+$  for these nucleophiles (Table 1) by extrapolation of the linear correlation between  $\log k_{\text{Nu}}$  for nucleophile addition to **1** and  $N_+$  shown in Figure 5A (open circles). The similar values of  $N_+ = 4.0$  determined here for iodide ion and  $N_+ = 4.7$  for glycylglycine is of particular interest because of the profoundly different Brønsted basicities of these nucleophiles and almost certainly reflects the particularly small intrinsic barrier for reaction of iodide ion.

There is no general agreement on why essentially constant nucleophile selectivities with changing electrophile reactivity are observed for reactions of strongly resonance-stabilized carbocations that follow the  $N_+$  scale (e.g., **2** and **3**),<sup>19,54b</sup> while sharp changes in selectivity for addition of substituted alkyl alcohols, alkyl carboxylates, and alkylamines are observed for changing reactivity of ring-substituted 1-phenylethyl carbocations<sup>48</sup> and 1-phenyl-2,2,2-trifluoroethyl carbocations.<sup>20</sup> This difference in reactivity–selectivity behavior requires that the position of the transition state for nucleophile addition to strongly resonance-stabilized carbocations remain essentially constant with changing thermodynamic driving force, but change relatively sharply with similar changes in thermodynamic driving force for nucleophile addition to 1-phenylethyl and 1-phenyl-2,2,2-trifluoroethyl carbocations. We have suggested that the small shifts in transition state structure for reactions of resonance-stabilized carbocations result from the large intrinsic barriers  $\Delta$  for these reactions (Scheme 7A), while the larger shifts in transition state structure for reactions of 1-phenylethyl and 1-phenyl 2,2,2-trifluoroethyl carbocations were proposed to reflect the relatively small intrinsic reaction barriers (Scheme 7B).<sup>20,22</sup>

A simple Marcus-type treatment of these data provides a useful framework for the description of these different structure–reactivity effects. The first derivative of the Marcus equation describes the fraction of a particular change in thermodynamic driving force that is expressed in the reaction transition state, and the second derivative describes how this fraction changes with changing driving force (eq 13).<sup>20,22,23</sup> A small value of the second derivative is predicted for reactions with a large intrinsic barrier that proceed through a transition state of nearly constant

(51) (a) Knier, B. L.; Jencks, W. P. *J. Am. Chem. Soc.* **1980**, *102*, 6789–6798. (b) McClelland, B. Personal communication.

(52) Pearson, R. G. *J. Am. Chem. Soc.* **1986**, *108*, 6109–6114.

(53) Pross, A. *Acc. Chem. Res.* **1985**, *18*, 212–219. Pross, A. In *Advances in Physical Organic Chemistry*; Academic Press: London, 1985; Vol. 21; pp 99–198.

(54) (a) Ritchie, C. D. *J. Am. Chem. Soc.* **1975**, *97*, 1170–1179. (b) Ritchie, C. D.; Tang, Y. *J. Org. Chem.* **1986**, *51*, 3555–3556.

Scheme 7

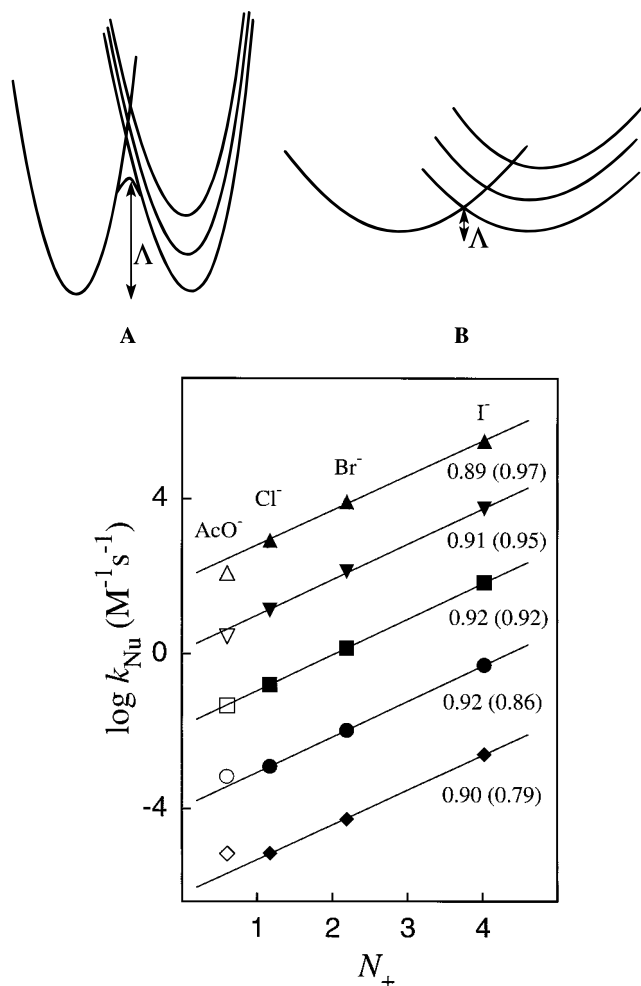


**Figure 7.** Logarithmic correlations of rate constants  $k_{\text{Nu}}$  ( $\text{M}^{-1} \text{s}^{-1}$ ) for addition of halide and acetate ions to **1** with the  $N_+$  value for the nucleophile (Table 1). The center correlation is the experimental data for the addition of halide and ions to **1** taken from Table 1. The upper and lower two correlations were constructed using hypothetical rate constants calculated from the Marcus equation (eq 11, derived at 298 K) with incremental 5 kcal/mol decreases and increases, respectively, in  $\Delta G^\circ$  for nucleophile addition to **1**, with the assumption that the values of  $\Lambda$  for these reactions (Table 2) remain constant. The numbers below each line are the slopes of the correlation for halide ions only, and the slopes of the correlations that include acetate ion are given in parentheses (see text).

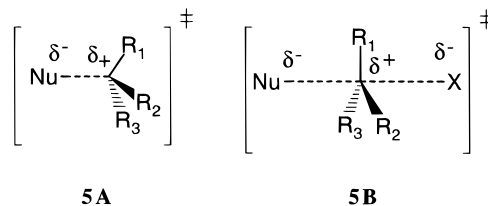
structure (Scheme 7A); an increase in the second derivative would result from a change to a smaller intrinsic barrier for a reaction that shows a larger change in transition-state structure with changing thermodynamic driving force (Scheme 7B).

$$\partial^2 \Delta G^\ddagger / \partial \Delta G^{\circ 2} = 1/8\Lambda \quad (13)$$

We have used the rate and equilibrium constants and intrinsic barriers for the addition of nucleophiles to **1** (Table 2) to calculate hypothetical changes in nucleophile selectivity for reactions that follow the Marcus equation (eq 11). The results of these calculations for nucleophilic addition reactions of acetate and halide ions to **1** are shown in Figure 7 where (a) the center correlation shows the experimental data for nucleophile addition to **1** (Table 1) and (b) the upper and lower two correlations were constructed using rate constants calculated from eq 11 with incremental 5 kcal/mol decreases and increases, respectively, in  $\Delta G^\circ$  for nucleophile addition to **1**, with the

assumption that the values of  $\Lambda$  for these reactions (Table 2) remain constant. The slopes of the correlation lines for the reactions of halide ions are given below each line. These slopes remain remarkably constant ( $s = 0.91 \pm 0.02$ ) for a 20 kcal/mol change in thermodynamic driving force for nucleophile addition, so that this simple Marcus analysis *predicts* no more than small changes in nucleophile selectivities for addition of halide ions to **1** with changing thermodynamic driving force. This analysis provides support for the conclusion that the constant selectivities observed for addition of a variety of nucleophiles to Ritchie electrophiles (e.g., **2** and **3**) are a consequence of the relatively large intrinsic barriers for these reactions.<sup>20,22</sup> A similar treatment of rate and equilibrium data for the reactions of the nucleophiles and electrophiles that were used in the construction of the  $N_+$  scale would be required to provide a more demanding test of this proposal.

The deviations of the rate constant for the reaction of acetate ion with **1** from the linear correlations for the reactions of halide ions shown in Figure 7 provide another example of how variations in intrinsic reaction barriers can lead to breakdowns in otherwise systematic structure–reactivity correlations.<sup>22,23</sup> The slopes of the correlations that include acetate ion increase from 0.79 to 0.97 (parentheses, Figure 7). However, these changes do not reflect an apparently anomalous shift to a transition state with greater covalent bond formation to the nucleophilic reagent with increasing thermodynamic driving force! Rather, they are due to the systematic drift in the point for acetate ion (open symbols) from above to below the correlation line for the reactions of halide ions with increasing thermodynamic driving force for nucleophile addition. This drift reflects the different effects of changes in  $\Delta G^\circ$  on the activation barrier  $\Delta G^\ddagger$  for the nucleophilic addition reactions of acetate and halide ions. In the case of the nearly thermoneutral but intrinsically difficult (large  $\Lambda$ ) reactions of acetate ion, about 50% of the change in  $\Delta G^\circ$  is expressed at the reaction transition state. By comparison, sharper changes in  $\Delta G^\ddagger$  with changing thermodynamic driving force are observed for the reactions of halide ions, because there is a significantly larger (>50%) expression of the changes in  $\Delta G^\circ$  in the transition state for these thermodynamically unfavorable, but intrinsically easy (small  $\Lambda$ ), reactions.



**The Ritchie and Swain–Scott Nucleophilicity Scales.** Our determination of rate constants for the addition of halide and acetate ions to **1** extends the Ritchie  $N_+$  scale to a  $10^8$ -fold span of nucleophile reactivity and allows for a broad comparison of Ritchie  $N_+$  nucleophilicity parameters for addition to  $\text{sp}^2$ -hybridized electrophilic carbon with Swain–Scott  $n$  parameters for bimolecular aliphatic nucleophilic displacement reactions in water.<sup>55–57</sup> Figure 5B shows that there is a good linear correlation with a slope of 2.0 ( $r = 0.98$ ) between the values of  $N_+$  and  $n$  for the reactions of all the nucleophiles examined here, except azide ion and nucleophiles with nonbonding electron pair(s) at atoms adjacent to the nucleophilic site ( $\alpha$ -effect nucleophiles). There is good agreement between the

(55) Swain, C. G.; Scott, C. B. *J. Am. Chem. Soc.* **1953**, *75*, 141–147.

(56) Koskikallio, J. *Acta Chem. Scand.* **1969**, *23*, 1477–1489.

(57) Pearson, R. G. *J. Org. Chem.* **1987**, *52*, 2131–2136.

correlation shown in Figure 5B and an earlier correlation (slope = 2.1) of Ritchie  $N_+$  ( $10^3$ -fold range of nucleophile reactivity) and Swain–Scott  $n$  values for primary and secondary amines.<sup>58</sup> The observation that the data for the addition of both anionic and neutral nucleophiles to charged (carbocations) and neutral (alkyl halides) electrophiles are correlated by a single line (Figure 5B) provides further evidence that Coulombic interactions between the electrophile and nucleophile do not have a significant effect on the relative order of nucleophile reactivity.<sup>59</sup>

The extended correlation in Figure 5B clearly defines the most important differences between nucleophilic reactivity toward  $sp^2$ -hybridized and  $sp^3$ -hybridized electrophilic carbon:

(1) The slope of 2.0 for the correlation line in Figure 5B shows that the rate constants for nucleophile addition to  $sp^2$ -hybridized carbon are twice as sensitive to changes in nucleophile reactivity as those for nucleophilic substitution at  $sp^3$ -hybridized carbon. This requires that there be a significantly larger fractional formation of the carbon–nucleophile bond at the transition state **5A** for addition to  $sp^2$ -hybridized electrophiles than at transition state **5B** for aliphatic nucleophilic substitution. The rate constants for nucleophilic substitution at the less selective methyl halides are significantly smaller than those for nucleophilic addition to the more selective electrophiles which follow the  $N_+$  scale. This is another violation of the reactivity-selectivity “principle”.<sup>60</sup> The observation that the activation barriers for formation of transition state **5A** are significantly lower than those for formation of transition state **5B** in which there is a smaller fractional bond formation to the reacting nucleophile shows that there is a much steeper rise in energy with development of a *fifth* bond to carbon at the pentavalent transition state **5B** for bimolecular aliphatic substitution, compared with development of a *fourth* bond to carbon at the tetravalent transition state **5A**. These results are in line with the expected difficulty of placing 10 bonding electrons at the central carbon.

(58) Bunting, J. W.; Mason, J. M.; Heo, C. K. *M. J. Chem. Soc., Perkin Trans. 2* **1994**, 2291–2300.

(59) Ritchie, C. D.; Sawada, M. *J. Am. Chem. Soc.* **1977**, 99, 3754–3761.

(60) For other examples of “failures” in the reactivity–selectivity principle see: Young, P. R.; Jencks, W. P. *J. Am. Chem. Soc.* **1979**, 101, 3288–3294.

(2) There are differences in the relative reactivity of  $\alpha$ -effect nucleophiles toward carbocations and alkyl halides.<sup>61</sup> The deviations for  $\alpha$ -effect nucleophiles reflect the well-known larger effect of nonbonding  $\alpha$ -electron pair(s) on nucleophile reactivity toward carbocations than in bimolecular aliphatic substitution reactions.<sup>61–65</sup> However, our data provide no additional insight into the origin(s) of the  $\alpha$ -effect, which has been the subject of intense, but not entirely conclusive, discussion.<sup>61,66–68</sup>

(3) The large positive deviation of the point for azide ion from the correlation in Figure 5B has been noted in earlier work, but also is not well understood.<sup>51a,69</sup>

**Acknowledgment.** We acknowledge the National Institutes of Health Grant GM 39754 for its generous support of this work and Tina L. Amyes for helpful discussion.

**Supporting Information Available:** A table of the observed second-order rate constants ( $k_{\text{Nu}}/\text{obsd}$  ( $\text{M}^{-1} \text{s}^{-1}$ )) for addition of anionic and neutral nucleophiles to **1** as a function of pH (data plotted in Figure 1). This material is available free of charge via the Internet at <http://pubs.acs.org>.

JA9937526

(61) Hoz, S.; Buncel, E. *Isr. J. Chem.* **1985**, 26, 313–319.

(62) Oae, S.; Kadoma, Y.; Yano, Y. *Bull. Chem. Soc. Jpn.* **1969**, 42, 1110–1112. McIsaac, J. E.; Subbaraman, L. R.; Mulhausen, H. A.; Behrman, E. J. *J. Org. Chem.* **1972**, 37, 1037–1041.

(63) Gregory, M. J.; Bruice, T. C. *J. Am. Chem. Soc.* **1967**, 89, 4400–4402.

(64) Zoltewicz, J. A.; Deady, L. W. *J. Am. Chem. Soc.* **1972**, 94, 2765–2769.

(65) Pearson, R. G.; Edgington, D. N. *J. Am. Chem. Soc.* **1962**, 84, 4607–4608.

(66) Ritchie, C. D.; Minasz, R. J.; Kamego, A. A.; Sawada, M. *J. Am. Chem. Soc.* **1977**, 99, 3747–3753. Sander, E. G.; Jencks, W. P. *J. Am. Chem. Soc.* **1968**, 90, 6154–6161. Dixon, J. E.; Bruice, T. C. *J. Am. Chem. Soc.* **1971**, 93, 3248–3254.

(67) Hoz, S. In *Nucleophilicity*; Harris, J. M., McManus, S. P., Eds.; American Chemical Society: Washington, DC, 1987; pp 181–193.

(68) Colthurst, M. J.; Kanagasooriam, A. J. S. S.; Wong, M. S. O.; Contini, C.; Williams, A. *Can. J. Chem.* **1978**, 56, 678–685.

(69) Amyes, T. L.; Jencks, W. P. *J. Am. Chem. Soc.* **1989**, 111, 7900–7909.

(70) Gandler, J. R. *J. Am. Chem. Soc.* **1985**, 107, 8218–8223.

(71) Ride, J. N.; Wyatt, P. A. H.; Zochowski, Z. M. *J. Chem. Soc., Perkin Trans. 2* **1974**, 1188–1189.

(72) Ritchie, C. D.; VanVerth, J. E.; Virtanen, P. O. I. *J. Am. Chem. Soc.* **1982**, 104, 3491–3497.